Weierstraß-Institut
für Angewandte Analysis und Stochastik

im Forschungsverbund Berlin e.V.

Preprint ISSN 0946 – 8633

Elastic half-plane under random boundary excitations

I.A. Shalimova [1] and K.K. Sabelfeld[1, 2]

[1] Institute of Computational Mathematics
and Mathematical Geophysics, Russian Acad. Sci.
Lavrentieva str.,6, 630090 Novosibirsk, Russia
[2] Weierstrass Institute for Applied Analysis and Stochastics,
Mohrenstrase 39. D – 10117 Berlin, Germany;
E-Mail: sabelfel@wias-berlin.de

No. 1314
Berlin 2008

1991 *Mathematics Subject Classification.* 65C05, 65C20, 65Z05.

Key words and phrases. White noise, Karhunen-Loève expansion, Poisson integral formula, boundary random excitations, 2D Lamé equation .

This work is supported partly by the RFBR Grant N 06-01-00498, HIII 4774.2006.1, and NATO Linkage Grant CLG 981426. I. Shalimova acknowledges the host institute WIAS and the support of DFG, a 3 months Grant of 2008.

Edited by
Weierstraß-Institut für Angewandte Analysis und Stochastik (WIAS)
Mohrenstraße 39
10117 Berlin
Germany

Fax: + 49 30 2044975
E-Mail: preprint@wias-berlin.de
World Wide Web: http://www.wias-berlin.de/

Abstract

We study in this paper a respond of an elastic half-plane to random boundary excitations. We treat both the white noise excitations and more generally, homogeneous random fluctuations of displacements prescribed on the boundary. Solutions to these problems are inhomogeneous random fields which are however homogeneous with respect to the longitudinal coordinate. This is used to represent the displacements as series expansions involving a complete set of deterministic functions with corresponding random coefficients. We construct the Karhunen-Loève (K-L) series expansion which is based on the eigen-decomposition of the correlation operator. The K-L expansion can be used to calculate the statistical characteristics of other functionals of interest, in particular, the strain and stress tensors and the elastic energy tensor.

1 Introduction.

Boundary value problems for PDEs with random coefficients and other stochastically fluctuating parameters are used in many fields of science and technology to describe uncertainty, probabilistic distribution of irregularities, or large ensembles of measurements under similar but randomly fluctuating conditions. The most famous example is the turbulence governed by a Navier-Stokes equation with stochastic source [16]. Stochastically driven Navier-Stokes equations with a stochastic forcing are studied intensively, they have very long history and interesting applications [3]. We mention here the analysis of synoptic meteorological data [14], and fundamental full developed turbulence study [15], where the Karhunen-Loève expansions are used.

Very well known is the example with flows in porous media and soils governed by the Darcy equation with a random hydraulic conductivity coefficient [2], [22], [11], as well as biological tissues [28], and in geodesy [19], [24]. In electrical impedance tomography [9] important problem is to evaluate a global response to random boundary excitations, and to estimate local fluctuations of the solution fields. Similar analysis is made in the inverse problems of elastography [18], [21], recognition technology [5], acoustic scattering from rough surfaces [27], fluid dynamics [1], and reaction-diffusion equations with white noise boundary perturbations [26].

It should be noted that most widely used are homogeneous Gaussian random field models because in this case, there are many convenient and efficient methods based on the spectral decomposition. Among those, we mention both deterministic and randomized spectral methods (e.g., see [25], [4], [20], [13], [12]).

The first study of random boundary excitations for the Laplace equation under random Dirichlet and Neumann boundary conditions, biharmonic equation, and the Lamé equation governing a 2D elastostatics problem for a disc, published by K. Sabelfeld in [21], is here extended to the case of an elastic half-plane.

The motivation to study the correlation structure of the displacement vector field of an elastic half-plane comes from different direct and inverse problems in structural mechanics [4], and

seismology [8], [30]. In the last paper, the Karhunen-Loève (K-L) expansion is applied to the separation of diffractions from reflections, for the model problem of a rigid half-plane. We mention also the problem of X-ray diffraction analysis of epitaxial layers [10]. The difference between lattice parameters of a desired epitaxial layer and that of available substrate crystals gives rise to elastic strains. The dislocation densities vary from several dislocations per sample at initial stages of the relaxation process to a dislocation per dozen lattice spacing in completely relaxed heteroepitaxial systems with large mismatch. In [12], the case of dislocations uniformly distributed on the boundary was studied. We construct an exact Karhunen-Loève expansion of the correlation tensor and the displacement vector field under white noise and general homogeneous random excitations on the boundary in the 2D elastostatics problem for a half-plane. It should be stressed that we give here the optimal orthogonal decomposition for the random vector of displacements which implies, that the method enables to construct Monte Carlo algorithm for calculation of statistical characteristics for any desired functional, e.g., the strain tensor, the elastic energy, etc. For illustration, we present some numerical analysis, and compare the calculations against the exact results.

2 The system of Lamé equations governing an elastic half-plane.

Let us consider the Dirichlet problem for the system of Lamé equations in the domain $D^+ \subset R^2$, the upper half-plane with the boundary $\Gamma = \{y : \ y = 0\}$:

$$\Delta \mathbf{u}(\mathbf{x}) + \alpha \, \mathrm{grad} \, \mathrm{div} \mathbf{u}(\mathbf{x}) = 0, \quad \mathbf{x} \in D^+, \quad \mathbf{u}(x') = \mathbf{g}(x') \quad x' \in \Gamma = \partial D^+, \tag{1}$$

where $\mathbf{u}(\mathbf{x}) = (u_1(x,y), u_2(x,y))^T$ is a column vector of displacements, and $\mathbf{g} = (g_1, g_2)^T$ is the vector of displacements prescribed on the boundary. The elastic constant α

$$\alpha = \frac{\lambda + \mu}{\mu}$$

is expressed through the Lamé constants of elasticity λ and μ.

2.1 Poisson formula for the upper half-plane

The Poisson formula for the problem (1) has the form (see Appendix)

$$\mathbf{u}(x,y) = \int\limits_{-\infty}^{\infty} K(x-x',y) Q(x-x',y) \mathbf{g}(x') \, d\, x' \ , \tag{2}$$

where

$$K(x-x',y) = \frac{y}{\pi((x-x')^2 + y^2)}$$

is the kernel of the well-known Poisson formula for the Laplace equation (e.g., see [21], [23]) and

$$Q(x-x',y) = \mathrm{I} + \frac{\beta}{(x-x')^2 + y^2} \begin{pmatrix} (x-x')^2 - y^2 & 2(x-x')y \\ 2(x-x')y & -((x-x')^2 - y^2) \end{pmatrix} \ , \tag{3}$$

where I is the identity matrix, and $\beta = \frac{\lambda+\mu}{\lambda+3\mu}$.

3 Stochastic boundary value problem.

3.1 Correlation tensor.

Assume the prescribed boundary displacements g_i, $i = 1, 2$ are homogeneous random processes. Then, the solution $\mathbf{u}(x, y)$ is a random field, and our goal is to find its main statistical characteristics, the correlation tensor, and to construct a simulation formula for the samples of $\mathbf{u}$. Here we note that from the Poisson formula (2) it can be easily found that $\langle \mathbf{u} \rangle = \langle \mathbf{g} \rangle$, so without loss of generality we assume that $\langle \mathbf{g} \rangle = 0$. For simplicity, we deal here with Gaussian random fields, so we suppose that g_i are Gaussian random processes, which implies due to (2) that $\mathbf{u}(x, y)$ is also a Gaussian random field. Then, this zero mean random field is uniquely defined by its correlation tensor.

By the Poisson formula (2) for $\mathbf{u}$, the correlation tensor $B_u(x_1, y_1; x_2, y_2)$ for the displacements can be written as follows

$$B_u(x_1, y_1; x_2, y_2) = \langle \mathbf{u}(x_1, y_1) \otimes \mathbf{u}(x_2, y_2) \rangle = \langle \mathbf{u}(x_1, y_1) \mathbf{u}^T(x_2, y_2) \rangle$$
$$= \int_{-\infty}^{\infty} \int_{-\infty}^{\infty} K(x_1 - x_1', y_1) K(x_2 - x_2', y_2) Q(x_1 - x_1', y_1) B_g(x_1'; x_2') Q^T(x_2 - x_2', y_2)\, dx_1'\, dx_2' \ .$$

We use here the notation $\otimes$ for the direct product of vectors $\mathbf{u}(x_1, y_1)$ and $\mathbf{u}(x_2, y_2)$, and $B_g(x_1; x_2)$ for the correlation tensor of the random boundary vector $\mathbf{g}$

$$B_g(x_1'; x_2') = \langle \mathbf{g}(x_1') \otimes \mathbf{g}(x_2') \rangle \ .$$

Let us consider the case when $\mathbf{g}$ is a white noise. This implies that

$$\{B_g(x_1'; x_2')\}_{ij} = \delta_{ij} \delta(x_1' - x_2') \ , \quad i, j = 1, 2 \ .$$

Here we use standard notations, δ_{ij} for the Kronecker symbol, and $\delta(x_1' - x_2')$ for the Dirac δ-function. In this case,

$$B_u(x_1, y_1; x_2, y_2) = \int_{-\infty}^{\infty} K(x_1 - x_1', y_1) K(x_2 - x_1', y_2) Q(x_1 - x_1', y_1) Q^T(x_2 - x_1', y_2)\, dx_1' \ .$$

To integrate the right-hand side we use the Fourier transformation. Let us take a change of variables $z = x_1' - x_2$, this yields

$$B_u(x_1, y_1; x_2, y_2)$$
$$= \int_{-\infty}^{\infty} K(x_1 - x_2 - z, y_1) K(-z, y_2) Q(x_1 - x_2 - z, y_1) Q^T(-z, y_2)\, dz \ ,$$

and here in turn we use a new variable $\tau = x_1 - x_2$:

$$B_u(x_1, y_1; x_2, y_2) = \int_{-\infty}^{\infty} K(\tau - z, y_1) Q(\tau - z, y_1) Q^T(-z, y_2) K(-z, y_2)\, dz \ . \tag{4}$$

To write the integral in the form of a convolution, we notice that $K(-z, y_2) = K(z, y_2)$, and define the matrix $Q_1(z, y_2)$ by $Q_1(z, y_2) = Q(-z, y_2)$,

$$Q_1(z, y_2) = Q(-z, y_2) = \mathrm{I} + \frac{\beta}{z^2 + y_2^2} \begin{pmatrix} z^2 - y_2^2 & -2zy_2 \\ -2zy_2 & -(z^2 - y_2^2) \end{pmatrix} \ .$$

From (4), which has a convolution form, it is seen that $B_u(x_1, y_1; x_2, y_2)$ depends on $\tau = x_1 - x_2$, so we will write $B_u(\tau, y_1, y_2)$ instead of $B_u(x_1, x_2; y_1, y_2)$. Thus the convolution (4) is written shortly as

$$B_u(\tau, y_1, y_2) = K(\tau, y_1)Q(\tau, y_1) * Q_1(z, y_2)K(z, y_2) \ .$$

The Fourier transform property for convolutions yields

$$F^{-1}[B_u] = F^{-1}[K(\tau, y_1)\, Q(\tau, y_1)]\, F^{-1}[K(z, y_2)\, Q_1(z, y_2)] \ . \tag{5}$$

So we have to find the inverse transforms $F^{-1}[KQ]$ and $F^{-1}[KQ_1]$. Using the next simple Fourier transform formulae (see Appendix)

$$\begin{aligned} F^{-1}[\frac{y}{\pi(\tau^2+y^2)}] &= e^{-|\xi|y}, \\ F^{-1}[\frac{\tau^2-y^2}{\pi(\tau^2+y^2)^2}] &= -|\xi|e^{-|\xi|y}, \\ F^{-1}[\frac{-2\tau y}{\pi(\tau^2+y^2)^2}] &= \imath\xi e^{-|\xi|y}, \end{aligned} \tag{6}$$

we get

$$F^{-1}[K(\tau, y_1)\, Q(\tau, y_1)] = \frac{1}{2\pi}\, e^{-|\xi|y_1}\Big(\mathrm{I} - \beta \begin{pmatrix} |\xi|y_1 & \imath\xi y_1 \\ \imath\xi y_1 & -|\xi|y_1 \end{pmatrix}\Big) \ . \tag{7}$$

and similar formula for $F^{-1}[KQ_1]$. As a result, we arrive at

$$F^{-1}[B_u] = e^{-|\xi|(y_1+y_2)}\Big(\mathrm{I} - \beta y_1 \begin{pmatrix} |\xi| & \imath\xi \\ \imath\xi & -|\xi| \end{pmatrix}\Big)\Big(\mathrm{I} - \beta y_2 \begin{pmatrix} |\xi| & -\imath\xi \\ -\imath\xi & -|\xi| \end{pmatrix}\Big) \ . \tag{8}$$

Note that we have taken the inverse Fourier transform of the correlation tensor with respect to only one variable, the coordinate x. This tensor is known as a partial spectral tensor (e.g., see [20]). Let us denote it by S_u:

$$S_u(\xi, y_1, y_2) = F^{-1}[B_u(\tau, y_1, y_2)] = \frac{1}{2\pi} \int_{-\infty}^{\infty} e^{-\mathrm{i}\xi\tau}\, B_u(\tau, y_1, y_2)\, d\tau \ .$$

It is convenient to introduce a matrix $S'(\xi, y_1, y_2)$ by $S' = e^{|\xi|(y_1+y_2)}S_u$, so from (8)

$$S' = \begin{pmatrix} 1 + 2\beta^2 y_1 y_2 \xi^2 - \beta|\xi|(y_1+y_2) & -\imath(\xi\beta(y_1-y_2) + 2\beta^2 y_1 y_2 \xi|\xi|) \\ \imath(-\xi\beta(y_1-y_2) + 2\beta^2 y_1 y_2 \xi|\xi|) & 1 + 2\beta^2 y_1 y_2 \xi^2 + \beta|\xi|(y_1+y_2) \end{pmatrix} . \tag{9}$$

So we will find now the correlation tensor B_u by using the relevant Fourier transform properties. Indeed, using the Fourier transform formulae (6) and (e.g., see [6])

$$\begin{aligned} F^{-1}[\frac{2(y_1+y_2)((y_1+y_2)^2-3\tau^2)}{\pi(\tau^2+(y_1+y_2)^2)^3}] &= \xi^2 e^{-|\xi|(y_1+y_2)}, \\ F^{-1}[\frac{2\tau(3(y_1+y_2)^2-\tau^2)}{\pi(\tau^2+(y_1+y_2)^2)^3}] &= -\imath\xi|\xi|e^{-|\xi|(y_1+y_2)}, \end{aligned}$$

we finally get from (8) and (9) the desired representation for the tensor B_u

$$\begin{aligned} B_u = {} & \frac{y_1+y_2}{\pi(\tau^2+(y_1+y_2)^2)}\,\mathrm{I} \\ & + \frac{\beta(y_1+y_2)}{\pi(\tau^2+(y_1+y_2)^2)^2} \begin{pmatrix} \tau^2-(y_1+y_2)^2 & 2\tau(y_1-y_2) \\ 2\tau(y_1-y_2) & -(\tau^2-(y_1+y_2)^2) \end{pmatrix} \\ & + \frac{4y_1y_2\beta^2}{\pi(\tau^2+(y_1+y_2)^2)^3} \begin{pmatrix} (y_1+y_2)((y_1+y_2)^2-3\tau^2) & \tau(3(y_1+y_2)^2-\tau^2) \\ -\tau(3(y_1+y_2)^2-\tau^2) & (y_1+y_2)((y_1+y_2)^2-3\tau^2) \end{pmatrix} . \end{aligned} \tag{10}$$

3.2 Spectral representations for partially homogeneous random fields.

So we deal with the case when the solution random field $\mathbf{u}(x,y)$ is homogeneous with respect to the variable x, it means that

$$B_u = \langle \mathbf{u}(x_1,y_1) \otimes \mathbf{u}(x_2,y_2) \rangle = B_u(x_1 - x_2, y_1, y_2) \ .$$

As mentioned above, the random fields with this property are called partially homogeneous random fields [20], with the partial spectral tensor

$$S_u(\xi, y_1, y_2) = \frac{1}{2\pi} \int\limits_{-\infty}^{\infty} B_u(\tau, y_1, y_2) e^{-\mathrm{i}\tau\xi} \, d\tau \ .$$

Randomization spectral methods are well developed for simulation of homogeneous random fields (e.g., see [25], [4], [20], [7]). They can be also applied to simulate partially homogeneous random fields $\mathbf{u}(x,y)$ as described in [20]. Here the random field $\mathbf{u}$ is homogeneous with respect to the first variable x, and inhomogeneous with respect to the second variable, y. The method enables to reduce the problem to a simulation of a inhomogeneous random field of smaller dimension, with respect to the second (inhomogeneous) variable y.

However in some special cases, when the partial spectral tensor $S_u(\xi, y_1, y_2)$ can be factorized in a product of the matrix G and its complex conjugate transpose, $G(y_1)G^*(y_2)$, the Randomization method can be also applied to reproduce the desired correlation tensor.

The Randomization spectral model for the partial homogeneous field presented in [20] has the form

$$\hat{\mathbf{u}}(x,y) = \frac{1}{[p(\xi)]^{1/2}} \Big[\zeta_\xi(y) \cos(\xi x) + \eta_\xi(y) \sin(\xi x) \Big], \tag{11}$$

where the random variable ξ has the distribution density $p(\xi)$ in the wave space, and a real-valued 4-dimensional field $(\zeta_\xi(y), \eta_\xi(y))^T$ for fixed ξ has the correlation tensor

$$\begin{aligned} B_{(\zeta,\eta)}(y_1,y_2) = \begin{pmatrix} \langle \zeta_\xi(y_1) \otimes \zeta_\xi(y_2) \rangle & \langle \zeta_\xi(y_1) \otimes \eta_\xi(y_2) \rangle \\ \langle \eta_\xi(y_1) \otimes \zeta_\xi(y_2) \rangle & \langle \eta_\xi(y_1) \otimes \eta_\xi(y_2) \rangle \end{pmatrix} &= \begin{pmatrix} \Re S_u(\xi,y_1,y_2) & \Im S_u(\xi,y_1,y_2) \\ -\Im S_u(\xi,y_1,y_2) & \Re S_u(\xi,y_1,y_2) \end{pmatrix} \\ &= e^{-|\xi|(y_1+y_2)} \begin{pmatrix} \Re S'(\xi,y_1,y_2) & \Im S'(\xi,y_1,y_2) \\ -\Im S'(\xi,y_1,y_2) & \Re S'(\xi,y_1,y_2) \end{pmatrix} . \end{aligned} \tag{12}$$

Here we use the notation $\Re S$ and $\Im S$ for the real and imaginary part of S, respectively. The probability density $p(\xi)$ is quite arbitrary but satisfies some natural weak conditions (see the discussion in [20] where it is suggested to take $p(\xi)$ proportional to the trace of the spectral matrix S_u).

The correlation tensor in the right-hand side of (12) is symmetric, $B_{(\zeta,\eta)}(y_1,y_2) = B^T_{(\zeta,\eta)}(y_2,y_1)$, and positive definite, see [20], p.39.

Now we decompose S'_u in a product, $S'_u = G(y_1)G^*(y_2)$, where G is the matrix from (7), i.e.,

$$G(y) = \mathrm{I} - \beta y \begin{pmatrix} |\xi| & \imath\xi \\ \imath\xi & -|\xi| \end{pmatrix} \ , \tag{13}$$

and the star sign stands for the complex conjugate transpose.

It is easy to verify that

$$\begin{pmatrix} \Re S_u & \Im S_u \\ -\Im S_u & \Re S_u \end{pmatrix} = e^{-|\xi|(y_1+y_2)} \begin{pmatrix} \Re G(y_1) & \Im G(y_1) \\ -\Im G(y_1) & \Re G(y_1) \end{pmatrix} \begin{pmatrix} \Re G(y_2) & \Im G(y_2) \\ -\Im G(y_2) & \Re G(y_2) \end{pmatrix}^T .$$

Then the 4-dimensional vector field $(\zeta_\xi(y), \eta_\xi(y))^T$ defined by

$$\begin{pmatrix} \zeta_\xi \\ \eta_\xi \end{pmatrix} = e^{-|\xi|y} \begin{pmatrix} \Re G & \Im G \\ -\Im G & \Re G \end{pmatrix} \begin{pmatrix} \zeta \\ \eta \end{pmatrix} , \tag{14}$$

where ζ and η are independent 2-dimensional Gaussian random vectors with zero mean and unit covariance matrix, has the desired correlation tensor (12).

Thus we have a Randomization spectral model of type (11) where the random vectors ζ_ξ and η_ξ are constructed by (14), and ξ is sampled according an arbitrary density p in the wave space.

This model has the desired correlation tensor, i.e., $B_{\hat{u}} = B_u$,

$$\begin{aligned} B_u(\tau, y_1, y_2) &= \int_{-\infty}^{\infty} S_u(\xi, y_1, y_2) e^{\mathrm{i}\tau\xi}\, d\xi \\ &= \int_{-\infty}^{\infty} \Big[\Re S_u(\xi, y_1, y_2) \cos(\xi\tau) - \Im S_u(\xi, y_1, y_2) \sin(\xi\tau) \Big]\, d\xi , \end{aligned} \tag{15}$$

here $\tau = x_1 - x_2$, (see [20]). To get (15) we used the fact that the real part, $\Re S_u$, is symmetric on the real line, i.e., $\Re S_u(\xi) = \Re S_u(-\xi)$, while $\Im S_u$ is antisymmetric, i.e., $\Im S_u(\xi) = -\Im S_u(-\xi)$.

Let us show that the model (11) has the desired correlation tensor. Indeed, by (11) and (14)

$$\begin{aligned} &\langle \hat{\mathbf{u}}(x_1, y_1) \otimes \hat{\mathbf{u}}(x_2, y_2) \rangle \\ &\quad = \Big\langle \frac{e^{-|\xi|(y_1+y_2)}}{p(\xi)} \Big((\Re G(y_1)\zeta + \Im G(y_1)\eta) \cos(\xi x_1) + (\Re G(y_1)\eta - \Im G(y_1)\zeta) \sin(\xi x_1) \Big) \\ &\qquad\qquad \otimes \Big((\Re G(y_2)\zeta + \Im G(y_2)\eta)^T \cos(\xi x_2) + (\Re G(y_2)\eta - \Im G(y_2)\zeta)^T \sin(\xi x_2) \Big) \Big\rangle \\ &\quad = \Big\langle \frac{e^{-|\xi|(y_1+y_2)}}{p(\xi)} \Big[\Big(\Re G(y_1) \Re G^T(y_2) \langle \zeta^2 \rangle + \Im G(y_1) \Im G^T(y_2) \langle \eta^2 \rangle \Big) \cos(\xi x_1) \cos(\xi x_2) \\ &\qquad + \Big(\Re G(y_1) \Re G^T(y_2) \langle \eta^2 \rangle + \Im G(y_1) \Im G^T(y_2) \langle \zeta^2 \rangle \Big) \sin(\xi x_1) \sin(\xi x_2) \\ &\qquad + \Big(\Re G(y_1) \Im G^T(y_2) \langle \eta^2 \rangle - \Im G(y_1) \Re G^T(y_2) \langle \zeta^2 \rangle \Big) \sin(\xi x_1) \cos(\xi x_2) \\ &\qquad - \Big(\Re G(y_1) \Im G^T(y_2) \langle \zeta^2 \Big\rangle + \Im G(y_1) \Re G^T(y_2) \langle \eta^2 \rangle \Big) \cos(\xi x_1) \sin(\xi x_2) \Big] \Big\rangle \\ &\quad = \Big\langle \frac{e^{-|\xi|(y_1+y_2)}}{p(\xi)} \Big[\Big(\Re G(y_1) \Re G^T(y_2) + \Im G(y_1) \Im G^T(y_2) \Big) \cos(\xi(x_1 - x_2)) \\ &\qquad\qquad + \Big(\Re G(y_1) \Im G^T(y_2) - \Im G(y_1) \Re G^T(y_2) \Big) \sin(\xi(x_1 - x_2)) \Big] \Big\rangle \\ &\quad = \int_{-\infty}^{\infty} \Big[\Re S'_u(\xi, y_1, y_2) \cos(\xi(x_1 - x_2)) - \Im S'_u(\xi, y_1, y_2) \sin(\xi(x_1 - x_2)) \Big] e^{-|\xi|(y_1+y_2)} d\xi \\ &\quad = \int_{-\infty}^{\infty} S_u(\xi, y_1, y_2) e^{\mathrm{i}(x_1 - x_2)\xi}\, d\xi = B_u(x_1 - x_2, y_1, y_2) . \end{aligned}$$

Here we used the fact that ζ and η are random vectors with a unit covariance matrix.

Concerning the sampling of the wave vectors, one of the simplest choice is a uniform distribution. Then however we have to cut-off the range where the wave number ξ is defined, say from $-R$ to R, R being large enough. In addition, to ensure that all the high-dimensional distributions of the model are close to Gaussian, one usually takes a sum of independent realizations of modes (11). In another version, one makes a partition of the wave number space into bins, and takes a sum of samples with wave number modes sampled independently within each bin [20].

This is generally different from a deterministic approximation of the stochastic integral representation of the random field with the correlation tensor (15) where the integration is taken from $-R$ to R. This leads to an approximation in the form

$$\mathbf{u}(x,y) \approx \frac{1}{\sqrt{R}} \sum_{k=1}^{\infty} e^{-\frac{\pi k y}{R}} \Big[\Big(\Re G_k(y)\zeta_k + \Im G_k(y)\eta_k \Big) \cos(\frac{\pi\, k\, x}{R}) + \Big(\Re G_k(y)\eta_k - \Im G_k(y)\zeta_k \Big) \sin(\frac{\pi\, k\, x}{R}) \Big] \tag{16}$$

where $G_k(y)$ is the matrix G defined in (13) with the value ξ taken as $\xi = \pi k/R$, and η_k, ζ_k are families of independent standard Gaussian vectors.

This model has a correlation tensor which is an approximation to the original correlation tensor B_u:

$$B_u(\tau, y_1, y_2) \approx \frac{1}{R} \sum_{k=1}^{\infty} e^{-\frac{\pi k}{R}(y_1+y_2)} \Big(\Re S'(\frac{\pi\, k}{R}, y_1, y_2) \cos(\frac{\pi\, k\, \tau}{R}) - \Im S'(\frac{\pi\, k}{R}, y_1, y_2) \sin(\frac{\pi\, k\, \tau}{R}) \Big) \ .$$

All these arguments are basically rigorous and use essentially the important properties that (1) the solution random field is partially homogeneous, and (2) the partial spectral tensor $S_u(\xi, y_1, y_2)$ can be represented as a product of two matrices, $G(y_1)$ and $G^*(y_2)$.

In the next section we treat the solution as a general inhomogeneous random field, and obtain the Karhunen-Loève expansion for the random field itself, and for its correlation tensor.

3.3 The Karhunen-Loève expansion.

The Karhunen-Loève expansion has the form (e.g., see [29], [17])

$$\mathbf{u}(\mathbf{x}) = \sum_{k=1}^{\infty} \sqrt{\lambda_k}\, \eta_k\, \mathbf{h}_k(\mathbf{x}) \ ,$$

where η_k is a family of random variables, λ_k and $\mathbf{h}_k(x)$ are the eigen-values and eigen-functions of the covariance operator B_u, i.e.,

$$\int B_u(\mathbf{x}_1, \mathbf{x}_2) h_k(\mathbf{x}_2) d\mathbf{x}_2 = \lambda_k h_k(\mathbf{x}_1) \ .$$

In our case $\mathbf{u}$ is partially homogeneous, that means, it is homogeneous with respect to the variable x, and is inhomogeneous with respect to y. It implies, that the correlation tensor depends on $\tau = x_1 - x_2$ and on both points, y_1 and y_2: $B_u = B(x_1 - x_2, y_1, y_2)$. Thus the eigen-value problem reads

$$\int_0^{\infty} \int_{-\infty}^{\infty} B_u(x_1 - x_2, y_1, y_2)\, \mathbf{h}_k(x_2, y_2)\, dx_2\, dy_2 = \lambda_k\, \mathbf{h}_k(x_1, y_1) \ . \tag{17}$$

For the correlation tensor the Karhunen-Loève expansion looks like

$$B_u(x_1 - x_2, y_1, y_2) = \sum_{k=1}^{\infty} \lambda_k \left(\mathbf{h}_k(x_1, y_1) \otimes \mathbf{h}_k(x_2, y_2) \right) .$$

For our domain D^+ we apply a cut-off integration, from $-R$ to R in the eigen-value problem, i.e., we solve the eigen-value problem

$$\int_0^{\infty} \int_{-R}^{R} B_u(x_2 - x_1, y_1, y_2)\, \mathbf{h}_k(x_2, y_2)\, dx_2\, dy_2 = \lambda_k\, \mathbf{h}_k(x_1, y_1), \tag{18}$$

where R is sufficiently large. In what follows and throughout the paper we preserve for simplicity the notation $\mathbf{u} = (u_1, u_2)^T$ and B_u for the problem with the introduced cut-off, that means the problem (1) is considered in the region $\{(x, y) : -R \le x \le R, \quad y > 0\}$.

Theorem. *The solution random field* $\mathbf{u}(x, y)$ *has the following Karhunen-Loève expansion*

$$\begin{pmatrix} u_1(x,y) \\ u_2(x,y) \end{pmatrix} = \frac{1}{\sqrt{R}} \sum_{k=1}^{\infty} e^{-\frac{\pi k}{R} y} \left\{ \begin{pmatrix} \lambda_{11}\big(\zeta_k \cos[\pi\, k\, x/R] + \tilde{\zeta}_k \sin[\pi\, k\, x/R]\big) \\ \lambda_{21}\big(\zeta_k \sin[\pi\, k\, x/R] - \tilde{\zeta}_k \cos[\pi\, k\, x/R]\big) \end{pmatrix} \right.$$
$$\left. + \begin{pmatrix} -\lambda_{12}\big(\eta_k \cos[\pi\, k\, x/R] - \tilde{\eta}_k \sin[\pi\, k\, x/R]\big) \\ \lambda_{22}\big(\eta_k \sin[\pi\, k\, x/R] + \tilde{\eta}_k \cos[\pi\, k\, x/R]\big) \end{pmatrix} \right\} , \tag{19}$$

where ζ_k, $\tilde{\zeta}_k$ *and* η_k, $\tilde{\eta}_k$ *are independent standard Gaussian random variables, and the coefficients* λ_{ij} *are explicitly given by*

$$\lambda_{11}(y, k) = 1 - \beta\, \frac{\pi\, k}{R} y \ , \quad \lambda_{12}(y, k) = \beta\, \frac{\pi\, k}{R} y \ , \tag{20}$$

$$\lambda_{22}(y, k) = 1 + \beta\, \frac{\pi\, k}{R} y \ , \quad \lambda_{21}(y, k) = \lambda_{12}(y, k) \ . \tag{21}$$

The correlation tensor is represented by the series

$$B_u = \frac{1}{R} \sum_{k=1}^{\infty} e^{-\frac{\pi\, k}{R}(y_1 + y_2)} \begin{pmatrix} \Lambda_{11} \cos \frac{\pi k (x_1 - x_2)}{R} & \Lambda_{12} \sin \frac{\pi k (x_1 - x_2)}{R} \\ \Lambda_{21} \sin \frac{\pi k (x_1 - x_2)}{R} & \Lambda_{22} \cos \frac{\pi k (x_1 - x_2)}{R} \end{pmatrix} \tag{22}$$

where

$$\begin{aligned} \Lambda_{11} &= \Lambda_{11}(y_1, y_2, k) = \lambda_{11}(y_1, k)\lambda_{11}(y_2, k) + \lambda_{12}(y_1, k)\lambda_{12}(y_2, k) \ , \\ \Lambda_{12} &= \Lambda_{12}(y_1, y_2, k) = -\lambda_{11}(y_1, k)\lambda_{21}(y_2, k) + \lambda_{12}(y_1, k)\lambda_{22}(y_2, k)) \ , \\ \Lambda_{21} &= \Lambda_{21}(y_1, y_2, k) = \lambda_{21}(y_1, k)\lambda_{11}(y_2, k) - \lambda_{22}(y_1, k)\lambda_{12}(y_2, k) \ , \\ \Lambda_{22} &= \Lambda_{22}(y_1, y_2, k) = \lambda_{21}(y_1, k)\lambda_{21}(y_2, k) + \lambda_{22}(y_1, k)\lambda_{22}(y_2, k) \ . \end{aligned}$$

Proof. The derivation of expansions (19) and (22) will immediately follow from the solution of the eigen-value problem for the correlation tensor (18).

To get the Karhunen-Loève expansions for $\mathbf{u}$ we split it into two independent random fields:

$$\mathbf{u}(x, y) = \mathbf{V}_1(x, y) + \mathbf{V}_2(x, y) \ . \tag{23}$$

Since $\mathbf{V}_1$ and $\mathbf{V}_2$ are independent, the correlation tensor can be represented in the form

$$B_u = \langle \mathbf{u}(x_1, y_1) \otimes \mathbf{u}(x_2, y_2) \rangle = \langle \mathbf{V}_1(x_1, y_1) \otimes \mathbf{V}_1(x_2, y_2) \rangle + \langle \mathbf{V}_2(x_1, y_1) \otimes \mathbf{V}_2(y_2, y_2) \rangle \ . \quad (24)$$

So we have to solve the eigen-value problems for the correlation tensors B_{V_1} and B_{V_1}

$$\int_0^\infty \int_{-R}^{R} B_{V_i}(x_2 - x_1, y_1, y_2)\, h_{i,k}(x_2, y_2)\, dx_2\, dy_2 = \lambda_{i,k}\, h_{i,k}(x_1, y_1), \quad (25)$$

for $i = 1, 2$.

In the following statement we solve these two eigen-value problems.

Lemma. *The eigen-value problems (25) have the following systems of solutions: the eigen-values*

$$\lambda_{1,2k-1} = \lambda_{1,2k} = \frac{(1 - \beta + \beta^2)R}{2\pi k} \ , \quad k = 1, 2, \dots$$

and corresponding eigen-functions,

$$h_{1,2k-1}(x, y) = \frac{e^{-\frac{\pi\, k y}{R}}}{\Delta_1} \begin{pmatrix} \lambda_{11}(y, k)\ \cos\ \frac{\pi\, k}{R} x \\ \lambda_{21}(y, k)\ \sin\ \frac{\pi\, k}{R} x \end{pmatrix} , \quad h_{1,2k}(x, y) = \frac{e^{-\frac{\pi\, k y}{R}}}{\Delta_1} \begin{pmatrix} \lambda_{11}(y, k)\ \sin\ \frac{\pi\, k}{R} x \\ -\lambda_{21}(y, k)\ \cos\ \frac{\pi\, k}{R} x \end{pmatrix} , \quad (26)$$

and eigen-values

$$\lambda_{2,2k-1} = \lambda_{2,2k} = \frac{(1 + \beta + \beta^2)R}{2\pi k} \ ,$$

with the relevant eigen-functions

$$h_{2,2k-1}(x, y) = \frac{e^{-\frac{\pi\, k y}{R}}}{\Delta_2} \begin{pmatrix} -\lambda_{12}(y, k)\ \cos\ \frac{\pi\, k}{R} x \\ \lambda_{22}(y, k)\ \sin\ \frac{\pi\, k}{R} x \end{pmatrix} , \quad h_{2,2k}(x, y) = \frac{e^{-\frac{\pi\, k y}{R}}}{\Delta_2} \begin{pmatrix} -\lambda_{12}(y, k)\ \sin\ \frac{\pi\, k}{R} x \\ -\lambda_{22}(y, k)\ \cos\ \frac{\pi\, k}{R} x \end{pmatrix} , \quad (27)$$

where

$$\Delta_1 = \frac{R\sqrt{1 - \beta + \beta^2}}{\sqrt{2\pi k}} \ , \quad \Delta_2 = \frac{R\sqrt{1 + \beta + \beta^2}}{\sqrt{2\pi k}} \ .$$

Here the subindexes $_1$ *and* $_2$ *stand for the first and second series of eigen-functions.*

Proof. Each of the four systems of the chosen functions (26), (27) is orthonormal, i.e.,

$$\int_{-\infty}^{\infty} \int_{-R}^{R} (\psi_k(x, y) \cdot \psi_l(x, y)) dy\, dx = \delta_{kl}$$

where we use for brevity the notation ψ_k for the functions of each of the four systems, $h_{1,2k-1}$, $h_{1,2k}$, $h_{2,2k-1}$, or $h_{2,2k}$, and δ_{kl} is the Kronecker symbol. Moreover, these vectors are pairwise orthogonal, i.e.,

$$\int_{-\infty}^{\infty} \int_{-R}^{R} (h_{1,2k-1}(x, y)\ \cdot\ h_{1,2k}(x, y))\, dy\, dx = 0, \quad \int_{-\infty}^{\infty} \int_{-R}^{R} (h_{2,2k-1}(x, y)\ \cdot\ h_{2,2k}(x, y))\, dy dx = 0$$

holds for $k = 1, 2 \ldots$. The normalization follows from

$$\begin{aligned}
\|h_{1,2k-1}\|^2 &= \frac{1}{\Delta_1^2} \int_0^\infty \int_{-R}^{R} (h_{1,2k-1}(x,y) \cdot h_{1,2k-1}(x,y))\, dx\, dy \\
&= \frac{1}{\Delta_1^2} \int_0^\infty \int_{-R}^{R} e^{-2y\xi_k} \Big[(1-\beta y|\xi_k|)^2 \cos^2(\xi_k x) + \beta^2 y^2 \xi_k^2 \sin^2(\xi_k x) \Big] dx\, dy \\
&= \frac{R}{\Delta_1^2} \int_0^\infty (1 - 2\beta y|\xi_k| + 2\beta^2 \xi_k^2 y^2)\, e^{-2y\xi_k}\, dy = \frac{R^2(1-\beta+\beta^2)}{2\pi k \Delta_1^2} = 1 \ ,
\end{aligned}$$

where we use the notation $\xi_k = \pi k/R$. Note that $\|h_{1,2k}\|^2 = \|h_{1,2k-1}\|^2$. Similar evaluations yield $\|h_{2,2k-1}\|^2 = \|h_{2,2k}\|^2 = \frac{R^2(1+\beta+\beta^2)}{2\pi k \Delta_2^2} = 1$.

Thus we conclude that we have two orthonormal systems of functions, the first one, $\{h_{1,2k-1}, h_{1,2k}\}$, $k = 1, 2 \ldots$, and the second one, $\{h_{2,2k-1},\ h_{2,2k}\}$, $k = 1, 2 \ldots$. It is not difficult to see that B_{V_1} has a bilinear expansion over the functions of the first system, and B_{V_2} is expanded in a series over the functions of the second system, i.e.,

$$B_{V_1} = \sum_{k=1}^{\infty} \lambda_{1,2k} \Big\{ h_{1,2k-1}(x_1,y_1) \otimes h_{1,2k-1}(x_2,y_2) + h_{1,2k}(x_1,y_1) \otimes h_{1,2k}(x_2,y_2) \Big\} \ , \tag{28}$$

and

$$B_{V_2} = \sum_{k=1}^{\infty} \lambda_{2,2k} \Big\{ h_{2,2k-1}(x_1,y_1) \otimes h_{2,2k-1}(x_2,y_2) + h_{2,2k}(x_1,y_1) \otimes h_{2,2k}(x_2,y_2) \Big\} \ . \tag{29}$$

From the general Hilbert-Schmidt theorem on the bilinear expansion of symmetric integral operators it follows that $\{h_{1,2k-1},\ h_{1,2k}\}$ and $\{h_{2,2k-1},\ h_{2,2k}\}$ solve the eigen-value problems

$$\int_0^\infty \int_{-R}^{R} B_{V_i}(x_1 - x_2, y_1, y_2)\, h_{i,k}(x_2,y_2)\, dx_2\, dy_2 = \lambda_{i,k}\, h_{i,k}(x_1,y_1), \tag{30}$$

for $i = 1, 2$, respectively. This can be derived directly by substituting (28) and (29) in (30), and carrying out the integration over $dx_2\, dy_2$ in (30) and using the orthonormality property. This procedure immediately gives also the expressions for the eigen-values.

Another way to find the eigen-values is the following. Let us introduce complex-valued vectors $H_{1,k}$ and $H_{2,k}$ by $H_{1,k} = h_{1,2k-1} + \imath h_{1,2k}$, and $H_{2,k} = h_{2,2k-1} + \imath h_{2,2k}$. From (26) and (27) we get

$$H_{1,k}(x,y) = e^{-\frac{\pi k y}{R}} e^{\imath \xi_k x} \begin{pmatrix} \lambda_{11}(y,k) \\ -\imath \lambda_{21}(y,k) \end{pmatrix} ,$$

and

$$H_{2,k}(x,y) = e^{-\frac{\pi k y}{R}} e^{\imath \xi_k x} \begin{pmatrix} -\lambda_{12}(y,k) \\ -\imath \lambda_{22}(y,k) \end{pmatrix} .$$

Since $\lambda_{i,2k-1} = \lambda_{i,2k}$, we can rewrite (25) in the form

$$\int_0^\infty \int_{-R}^{R} B_{V_i}(x_1 - x_2, y_1, y_2)\, H_{i,k}(x_2,y_2)\, dx_2\, dy_2 = \lambda_{i,2k}\, H_{i,k}(x_1,y_1) \ , \quad i = 1, 2 \ . \tag{31}$$

Let us first consider this eigen-value problem for B_{V_1}. Substituting $H_{1,k}$ we find that

$$\int_0^\infty \int_{-R}^{R} B_{V_1}(x_1 - x_2, y_1, y_2) e^{-\frac{\pi\, k y_2}{R}} e^{\imath \xi x_2} \begin{pmatrix} \lambda_{11}(y_2,k) \\ -\imath\lambda_{21}(y_2,k) \end{pmatrix} dx_2 dy_2 = \lambda_{1,2k}\, e^{-\frac{\pi\, k y_1}{R}} e^{\imath\xi x_1} \begin{pmatrix} \lambda_{11}(y_1,k) \\ -\imath\lambda_{21}(y_1,k) \end{pmatrix},$$

or

$$\int_0^\infty \int_{-R}^{R} e^{-\imath\xi(x_1-x_2)} B_{V_1}(x_1 - x_2, y_1, y_2)\, dx_2 \begin{pmatrix} \lambda_{11}(y_2,k) \\ -\imath\lambda_{21}(y_2,k) \end{pmatrix} e^{-\frac{\pi\, k(y_2-y_1)}{R}}\, dy_2 = \lambda_{1,2k} \begin{pmatrix} \lambda_{11}(y_1,k) \\ -\imath\lambda_{21}(y_1,k) \end{pmatrix}.$$

We notice that the inner integral can be approximated by the relevant value of the spectral tensor

$$S_{V_1}(\xi, y_1, y_2) = \int_{-\infty}^{\infty} e^{-\imath\xi\tau} B_{V_1}(\tau, y_1, y_2)\, d\tau\ .$$

Therefore,

$$S_{V_1}(\xi, y_1, y_2) \approx S_{V_1}(\xi_k, y_1, y_2) = \int_{-R}^{R} e^{-\imath\xi_k\tau} B_{V_1}(\tau, y_1, y_2)\, d\tau\ , \quad \xi_k = \pi\, k/R\ .$$

The spectral tensor S_{V_1} has the form

$$\begin{aligned} S_{V_1}(\xi_k, y_1, y_2) &= e^{-|\xi_k|(y_1+y_2)} \times \\ &\begin{pmatrix} 1 + \beta^2 y_1 y_2 \xi_k^2 - \beta|\xi_k|(y_1+y_2) & -\imath(\xi_k\beta(y_1-y_2) + \beta^2 y_1 y_2 \xi_k|\xi_k|) \\ \imath(-\xi_k\beta(y_1-y_2) + \beta^2 y_1 y_2 \xi_k|\xi_k|) & \beta^2 y_1 y_2 \xi_k^2 \end{pmatrix}. \end{aligned} \tag{32}$$

We decompose S_{V_1} as $S_{V_1} = e^{-|\xi_k|(y_1+y_2)} G(y_1,\xi_k) G_1(y_2,\xi_k)$ where $G(y_1)$ is defined by (13), and $G_1(y_2)$ is defined by

$$G_1(y_2,\xi_k) = \begin{pmatrix} 1 - \beta|\xi_k| y_2 & \imath\xi_k\beta y_2 \\ 0 & 0 \end{pmatrix}\ , \tag{33}$$

hence

$$\int_0^\infty G(y_1,\xi_k) G_1(y_2,\xi_k)\, e^{-\frac{2\pi\, k y_2}{R}} \begin{pmatrix} \lambda_{11}(y_2,k) \\ -\imath\lambda_{21}(y_2,k) \end{pmatrix} dy_2 = \lambda_{1,2k} \begin{pmatrix} \lambda_{11}(y_1,k) \\ -\imath\lambda_{21}(y_1,k) \end{pmatrix}\ .$$

Multiplying both sides of the last equation by

$$G^{-1}(y_1,\xi_k) = \big(\mathrm{I} + \beta y_1 \begin{pmatrix} |\xi_k| & \imath\xi_k \\ \imath\xi_k & -|\xi_k| \end{pmatrix}\big)$$

we arrive at

$$\int_0^\infty G_1(y_2,\xi_k)\, e^{-\frac{2\pi\, k y_2}{R}} \begin{pmatrix} \lambda_{11}(y_2,k) \\ -\imath\lambda_{21}(y_2,k) \end{pmatrix} dy_2 = \lambda_{1,2k}\, G^{-1}(y_1,\xi_k) \begin{pmatrix} \lambda_{11}(y_1,k) \\ -\imath\lambda_{21}(y_1,k) \end{pmatrix}\ .$$

Substituting λ_{ij} from (20)-(21) yields

$$\int_0^\infty e^{-\frac{2\pi\, k y_2}{R}} \begin{pmatrix} 1 - 2\beta\xi_k y_2 + 2\beta^2\xi_k^2 y_2^2 \\ 0 \end{pmatrix} dy_2 = \lambda_{1,2k} \begin{pmatrix} 1 \\ 0 \end{pmatrix} .$$

After integration we get the result

$$\lambda_{1,2k} = \frac{1 - \beta + \beta^2}{2\xi_k} . \tag{34}$$

For the second series of eigen-vectors we obtain analogous formula

$$\int_0^\infty e^{-\frac{2\pi\, k y_2}{R}} \begin{pmatrix} 0 \\ -\imath(1 + 2\beta\xi_k y_2 + 2\beta^2\xi_k^2 y_2^2) \end{pmatrix} dy_2 = \lambda_{2,k} \begin{pmatrix} 0 \\ -\imath \end{pmatrix} ,$$

hence

$$\lambda_{2,2k} = \frac{1 + \beta + \beta^2}{2\xi_k} . \tag{35}$$

The proof of Lemma is complete. □

The expansions given in Theorem follow now from Lemma and the splittings (23) and (24). □

3.4 Simulation results for the white noise excitations.

To test the K-L expansions (19) for the displacements obtained in Theorem, we have carried out calculations of the correlation tensor by averaging the relevant products $u_i\, u_j$, $i = 1, 2$ over 10000 samples of (19), and compared the results with the exact expressions given by (10). In Figure 1 we present this comparison for the longitudinal B_{11} and transverse B_{22} correlation functions versus the longitudinal coordinate x, for $\alpha = 1/3$, and fixed heights $y_1 = y_2 = 1$ (left panel), and transverse coordinate y ($\alpha = 2$, right panel). The cut-off parameter was taken as $R = 100$, and the number of harmonics $n = 100$. The maximum error (for small values of x and y) was about one percent which was however easily decreased by increasing the parameter R to 300, and n to 200.

Note that the elasticity parameter α affects much the behaviour of the correlations. In Figure 2 (left panel) we show the same curves that are given in Figure 1 (left panel), but for $\alpha = \infty$. It is seen that the characteristic correlation lengths are decreased about two times compared to the case $\alpha = 1/3$, while the fluctuation intensities are increased about 3 times for the transverse correlations, and only 1.5 times for the longitudinal correlations.

In the right panel of Figure 2 the cross-correlations B_{12} and B_{21} versus the longitudinal coordinate x are plotted for $\alpha = \infty$, at the heights $y_1 = y_2$. It is seen that for correlations less than about ± 0.001 the accuracy is high, while after $x \sim 3$ the simulated curves begin to oscillate.

To see how the elasticity parameter affects the cross-correlations we present in Figure 3 the functions $B_{12}(x)$ and $B_{21}(x)$ at the height $y_1 = y_2 = 1$, for different values of α. The sensitivity analysis clearly shows that the elasticity parameter α can be easily recovered from the behaviour of the functions $B_{12}(x)$ and $B_{21}(x)$ which is a typical inverse problem in elastography (e.g., see [18]).

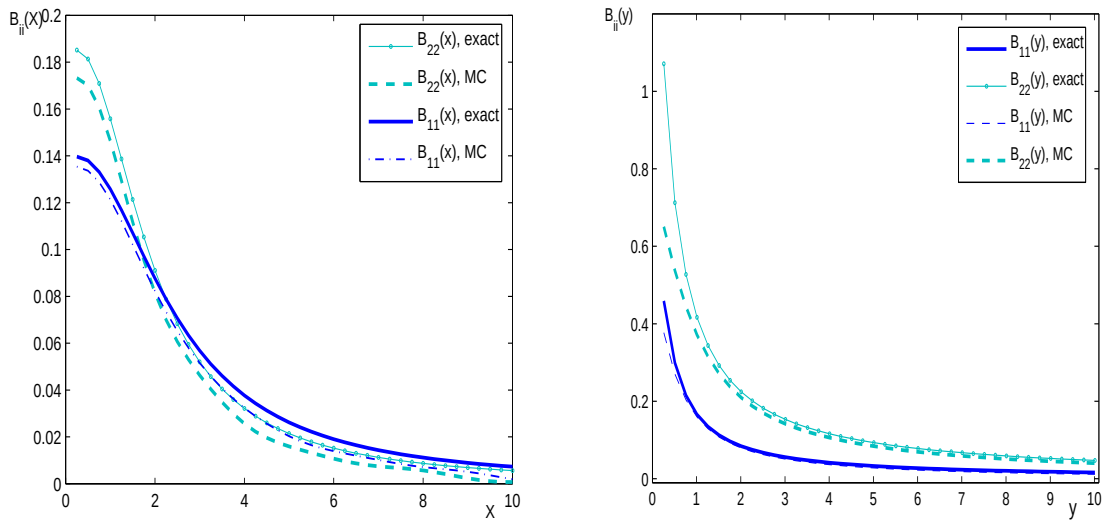

Figure 1: Comparison of the Monte Carlo simulations (MC) against the exact result for the case of white noise boundary excitations. The longitudinal B_{11} and transverse B_{22} correlation functions versus the longitudinal coordinate x ($\alpha = 1/3$, $y_1 = y_2 = 1$, left panel), and transverse coordinate y ($\alpha = 2$, right panel).

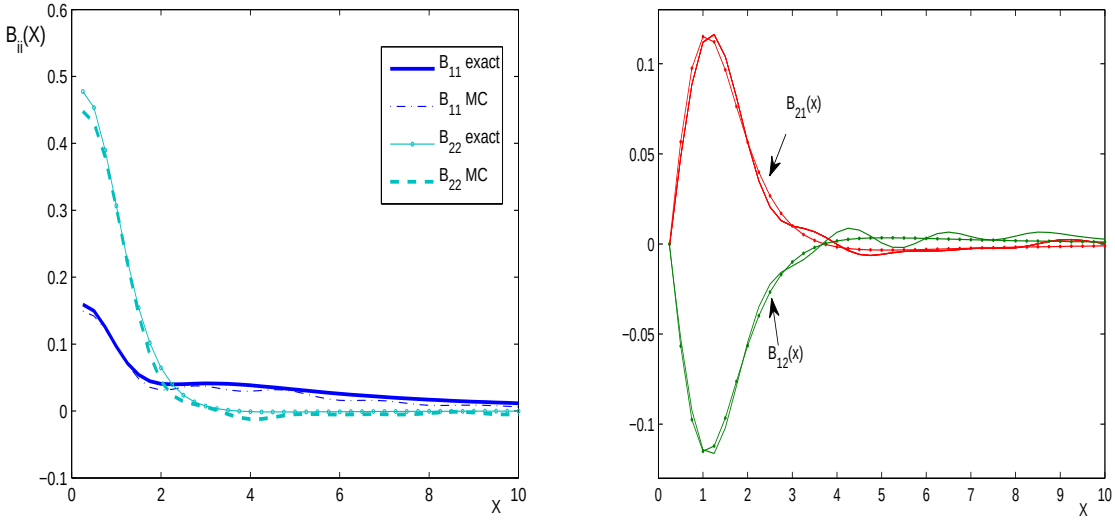

Figure 2: Comparison of the Monte Carlo simulations (MC) against the exact result for the case of white noise boundary excitations. The longitudinal B_{11} and transverse B_{22} correlation functions (left panel), and the cross-correlations B_{12} and B_{21} (right panel) versus the longitudinal coordinate x, for $\alpha = \infty$, $y_1 = y_2 = 1$, and $R = 100$.

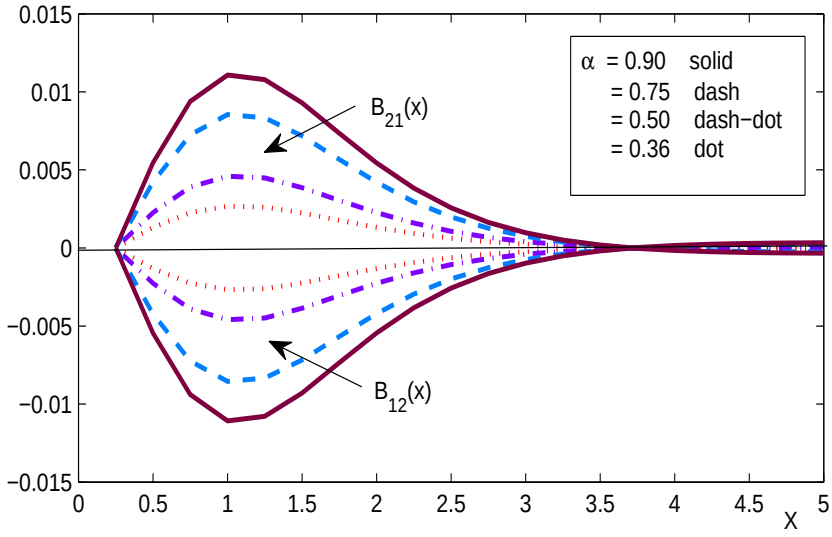

Figure 3: Sensitivity analysis for the case of white noise boundary excitations: the cross-correlations B_{12} and B_{21} versus the longitudinal coordinate x, for different values of α.

4 Homogeneous excitations.

Let us consider the boundary value problem (1) when $\mathbf{g}$ is a zero mean Gaussian vector random process with the correlation matrix

$$B_g(x_1';x_2') = \langle \mathbf{g}(x_1') \otimes \mathbf{g}(x_2') \rangle \ .$$

Then by the Poisson formula (2) for $\mathbf{u}(x,y)$

$$\begin{aligned} B_u(x_1,y_1;x_2,y_2) &= \langle \mathbf{u}(x_1,y_1) \otimes \mathbf{u}(x_2,y_2) \rangle \\ &= \int\limits_{-\infty}^{\infty} \int\limits_{-\infty}^{\infty} K(x_1-x_1',y_1) Q(x_1-x_1',y_1) B_g(x_1';x_2') K(x_2-x_2',y_2) Q^T(x_2-x_2',y_2)\, dx_1'\, dx_2'. \end{aligned} \quad (36)$$

Now we consider the case when $B_g(x_1';x_2')$ is homogeneous, it means that $B_g(x_1';x_2') = B_g(\tau')$, where $\tau' = x_1' - x_2'$. The relevant spectral tensor S_g is related to B_g by

$$B_g(\tau') = F[S_g] = \int\limits_{-\infty}^{\infty} e^{\imath\tau'\xi} S_g(\xi)\, d\xi, \quad S_g(\xi) = F^{-1}[B_g] = \frac{1}{2\pi} \int\limits_{-\infty}^{\infty} e^{-\imath\tau'\xi} B_g(\tau')\, d\tau' \ . \quad (37)$$

From (36) and (37), we obtain, using the change the variables $x_1' = \tau' + x_2'$,

$$\begin{aligned} B_u(x_1,y_1;x_2,y_2) = \int\limits_{-\infty}^{\infty} d\xi \int\limits_{-\infty}^{\infty} dx_2' \Big[\int\limits_{-\infty}^{\infty} d\tau' K(x_1-x_2'-\tau',y_1) Q(x_1-x_2'-\tau',y_1) e^{\imath\tau'\xi} \Big] \\ \times S_g(\xi) K(x_2-x_2',y_2) Q_1^T(x_2-x_2',y_2) \ . \end{aligned} \quad (38)$$

Now taking the new variable $z = x_1 - x_2' - \tau'$ we get

$$B_u(x_1, y_1; x_2, y_2) = \int_{-\infty}^{\infty} d\xi \; F^{-1}[KQ](\xi, y_1) S_g(\xi) \times \int_{-\infty}^{\infty} K(x_2 - x_2', y_2) Q_1^T(x_2 - x_2', y_2) e^{\imath(x_1 - x_2')\xi} \, dx_2' \; . \tag{39}$$

Using the change of variable $z_1 = x_2 - x_2'$ we finally arrive at

$$B_u(x_1, y_1; x_2, y_2) = \int_{-\infty}^{\infty} F^{-1}[KQ](\xi, y_1) S_g(\xi) F^{-1}[KQ_1^T](\xi, y_2) e^{\imath(x_1 - x_2)\xi} \, d\xi \; . \tag{40}$$

From the last formula we see that the correlation tensor B_u depends on the difference $x_1 - x_2$, i.e. **u** is partially homogeneous, with the partial spectral tensor

$$S_u(\xi) = F^{-1}[KQ](\xi, y_1) S_g(\xi) F^{-1}[KQ_1^T](\xi, y_2) \; .$$

Inserting the explicit form (7) we rewrite it as follows:

$$S_u(\xi) = e^{-|\xi|(y_1+y_2)} \Big(\mathrm{I} - \beta y_1 \begin{pmatrix} |\xi| & \imath\xi \\ \imath\xi & -|\xi| \end{pmatrix} \Big) S_g(\xi) \Big(\mathrm{I} - \beta y_2 \begin{pmatrix} |\xi| & -\imath\xi \\ -\imath\xi & -|\xi| \end{pmatrix} \Big) \; . \tag{41}$$

Notice that in the case of a white noise S_g is an identity matrix, (41) becomes (8).

To express B_u through B_g, we substitute the representation (37) in (40)

$$B_u(\tau, y_1, y_2) = \int_{-\infty}^{\infty} \int_{-\infty}^{\infty} e^{-|\xi|(y_1+y_2)} \times \Big(\mathrm{I} - \beta y_1 \begin{pmatrix} |\xi| & \imath\xi \\ \imath\xi & -|\xi| \end{pmatrix} \Big) B_g(\tau') \Big(\mathrm{I} - \beta y_2 \begin{pmatrix} |\xi| & -\imath\xi \\ -\imath\xi & -|\xi| \end{pmatrix} \Big) e^{\imath(\tau - \tau')\xi} \, d\xi \, d\tau' \; . \tag{42}$$

We introduce a new notation by arranging the entries of the correlation tensor in a 4-dimensional column vector. This notation is convenient when expressing the relation between the correlation tensors B_u and B_g. Let $\hat{B}_u = (B_{u,11}, B_{u,12}, B_{u,21}, B_{u,22})^T$, and $\hat{B}_g = (B_{g,11}, B_{g,12}, B_{g,21}, B_{g,22})^T$.

The representation (42) can be conveniently rewritten in the form

$$\hat{B}_u(\tau, y_1, y_2) = \int_{-\infty}^{\infty} A(\tau, \tau', y_1, y_2) \hat{B}_g(\tau') \, d\tau'$$

where

$$A(\tau, \tau', y_1, y_2)_{4\times 4} = \int_{-\infty}^{\infty} e^{-|\xi|(y_1+y_2)} \times \Big(\mathrm{I} - \beta y_1 \begin{pmatrix} |\xi| & \imath\xi \\ \imath\xi & -|\xi| \end{pmatrix} \Big) \otimes \Big(\mathrm{I} - \beta y_2 \begin{pmatrix} |\xi| & -\imath\xi \\ -\imath\xi & -|\xi| \end{pmatrix} \Big) e^{\imath(\tau - \tau')\xi} \, d\xi \; . \tag{43}$$

Here we denote by $\otimes$ a tensor product of two matrices which is defined in our case as a 4×4 matrix represented as a 2×2 block matrix each block being a 2×2 matrix of the form $G_{ij} \, G^*$, $i, j = 1, 2$, where G is defined in (13).

The entries a_{ij}, $i,j=1,\dots,4$ can be evaluated explicitly. Since the matrix A is symmetric we present the entries a_{ij} with $j \geq i$. We denote for simplicity $\Delta\tau = \tau - \tau'$,

$$
\begin{aligned}
a_{11} &= F[e^{-|\xi|(y_1+y_2)}(1-\beta y_1|\xi|)(1-\beta y_2|\xi|)] \\
&= \frac{y_1+y_2}{\pi((\Delta\tau)^2+(y_1+y_2)^2)}\Big[1+\beta\frac{(\Delta\tau)^2-(y_1+y_2)^2}{((\Delta\tau)^2+(y_1+y_2)^2)}+2\beta^2 y_1y_2\frac{(y_1+y_2)^2-3(\Delta\tau)^2}{((\Delta\tau)^2+(y_1+y_2)^2)^2}\Big] ,
\end{aligned}
$$

$$
\begin{aligned}
a_{12} &= F[e^{-|\xi|(y_1+y_2)}(1-\beta y_1|\xi|)\beta\imath y_2\xi] \\
&= -2\beta y_2\frac{(\Delta\tau)(y_1+y_2)}{\pi((\Delta\tau)^2+(y_1+y_2)^2)^2}+2\beta^2 y_1y_2\frac{(\Delta\tau)(3(y_1+y_2)^2-(\Delta\tau)^2)}{\pi((\Delta\tau)^2+(y_1+y_2)^2)^3} ,
\end{aligned}
$$

$$
\begin{aligned}
a_{13} &= F[e^{-|\xi|(y_1+y_2)}(-\beta y_1\xi)(1-\beta\imath y_2|\xi|)] \\
&= 2\beta y_1\frac{(\Delta\tau)(y_1+y_2)}{\pi((\Delta\tau)^2+(y_1+y_2)^2)^2}-2\beta^2 y_1y_2\frac{(\Delta\tau)(3(y_1+y_2)^2-(\Delta\tau)^2)}{\pi((\Delta\tau)^2+(y_1+y_2)^2)^3} ,
\end{aligned}
$$

$$
a_{14} = a_{23} = F[e^{-|\xi|(y_1+y_2)}\beta^2 y_1y_2\xi^2] = 2\beta^2 y_1y_2\frac{(y_1+y_2)((y_1+y_2)^2-3(\Delta\tau)^2)}{\pi((\Delta\tau)^2+(y_1+y_2)^2)^3} ,
$$

$$
\begin{aligned}
a_{22} = a_{33} &= F[e^{-|\xi|(y_1+y_2)}(1-\beta y_1|\xi|)(1+\beta y_2|\xi|)] \\
&= \frac{y_1+y_2}{\pi((\Delta\tau)^2+(y_1+y_2)^2)}+\beta(y_1-y_2)\frac{(\Delta\tau)^2-(y_1+y_2)^2}{\pi((\Delta\tau)^2+(y_1+y_2)^2)} \\
&\qquad -2\beta^2 y_1y_2\frac{(y_1+y_2)((y_1+y_2)^2-3(\Delta\tau)^2)}{\pi((\Delta\tau)^2+(y_1+y_2)^2)^3} ,
\end{aligned}
$$

$$
\begin{aligned}
a_{24} &= F[e^{-|\xi|(y_1+y_2)}(-\beta y_1\xi\imath)(1+\beta y_2|\xi|)] \\
&= 2\beta y_1\frac{(\Delta\tau)(y_1+y_2)}{\pi((\Delta\tau)^2+(y_1+y_2)^2)^2}+2\beta^2 y_1y_2\frac{(\Delta\tau)(3(y_1+y_2)^2-(\Delta\tau)^2)}{\pi((\Delta\tau)^2+(y_1+y_2)^2)^3} ,
\end{aligned}
$$

$$
\begin{aligned}
a_{34} &= F[e^{-|\xi|(y_1+y_2)}(1+\beta y_1|\xi|)\beta\imath y_2|\xi|] \\
&= -2\beta y_2\frac{(\Delta\tau)(y_1+y_2)}{\pi((\Delta\tau)^2+(y_1+y_2)^2)^2}-2\beta^2 y_1y_2\frac{(\Delta\tau)(3(y_1+y_2)^2-(\Delta\tau)^2)}{\pi((\Delta\tau)^2+(y_1+y_2)^2)^3} ,
\end{aligned}
$$

$$
\begin{aligned}
a_{44} &= F[e^{-|\xi|(y_1+y_2)}(1+\beta y_1|\xi|)(1+\beta y_2|\xi|)] \\
&= \frac{y_1+y_2}{\pi((\Delta\tau)^2+(y_1+y_2)^2)}\Big[1-\beta\frac{(\Delta\tau)^2-(y_1+y_2)^2}{((\Delta\tau)^2+(y_1+y_2)^2)}+2\beta^2 y_1y_2\frac{(y_1+y_2)^2-3(\Delta\tau)^2}{((\Delta\tau)^2+(y_1+y_2)^2)^2}\Big] .
\end{aligned}
$$

Let us consider the case when the zero mean boundary Gaussian random process $\mathbf{g}$ is given by the spectral expansion of its correlation tensor

$$
B_g = \frac{1}{R}\sum_{k=1}^{\infty} e^{-\imath\tau\xi_k} S_g(\xi_k) , \tag{44}
$$

where

$$
S_g(\xi_k) = \frac{1}{2\pi}\int_{-R}^{R} e^{-\imath\tau'\xi_k} B_g(\tau)\, d\tau', \quad \xi_k = \frac{\pi k}{R} . \tag{45}
$$

Using the representation (41) and the cut-off integration, and take ξ_k instead of ξ, we get the series expansion for the correlation tensor B_u:

$$B_u = \frac{1}{R}\sum_{k=1}^{\infty} e^{-\imath\tau\xi_k} S_u(\xi_k)$$
$$= \frac{1}{R}\sum_{k=1}^{\infty} e^{-\imath\tau\xi_k} e^{-\xi_k(y_1+y_2)} \Big(\mathrm{I} - \beta y_1 \begin{pmatrix} \xi_k & \imath\xi_k \\ \imath\xi_k & -\xi_k \end{pmatrix}\Big) S_g(\xi_k) \Big(\mathrm{I} - \beta y_2 \begin{pmatrix} \xi_k & -\imath\xi_k \\ -\imath\xi_k & -\xi_k \end{pmatrix}\Big). \quad (46)$$

4.1 Finite correlation length boundary excitations.

In this section we analyze an exact solvable example with boundary excitations having a finite correlation length.

So let us consider the boundary problem (1) when the homogeneous Gaussian random process **g** is defined by the following correlation tensor

$$B_g(\tau') = \begin{pmatrix} \sigma_1/((\frac{\tau'}{L_1})^2+1) & 0 \\ 0 & \sigma_2/((\frac{\tau'}{L_2})^2+1) \end{pmatrix}$$

where σ_1 and σ_2 are the fluctuation intensities, and L_1 and L_2 are the correlation lengths of g_1 and g_2, respectively. Its spectral tensor can be easily evaluated

$$S_g(\xi) = \begin{pmatrix} \sigma_1 L_1\, e^{-|\xi|L_1} & 0 \\ 0 & \sigma_2 L_2\, e^{-|\xi|L_2} \end{pmatrix}. \quad (47)$$

Now we substitute S_g in (40) and carry out the integration explicitly. This yields

$$\begin{aligned} B_u(\tau,y_1,y_2)_{11} &= a^1_{11}(1) + a^2_{11}(1) + a^3_{11}(1) + a^3_{11}(2) \\ B_u(\tau,y_1,y_2)_{12} &= a^1_{21}(1)y_2 + a^2_{21}(1) - a^1_{21}(2)y_1 + a^2_{21}(2) \\ B_u(\tau,y_1,y_2)_{21} &= -a^1_{21}(1)y_1 - a^2_{21}(1) + a^1_{21}(2)y_2 - a^2_{21}(2) \\ B_u(\tau,y_1,y_2)_{22} &= a^3_{11}(1) + a^1_{11}(2) - a^2_{11}(2) + a^3_{11}(2) \end{aligned} \quad (48)$$

where

$$\begin{aligned} a^1_{11}(i) &= L_i\sigma_i \frac{y_1+y_2+L_i}{\pi(\tau^2+(y_1+y_2+L_i)^2)}, \\ a^2_{11}(i) &= L_i\sigma_i\beta(y_1+y_2)\frac{\tau^2-(y_1+y_2+L_i)^2}{\pi(\tau^2+(y_1+y_2+L_i)^2)^2}, \\ a^3_{11}(i) &= 2L_i\sigma_i\beta^2 y_1y_2(y_1+y_2+L_i)\frac{(y_1+y_2+L_i)^2-3\tau^2}{\pi(\tau^2+(y_1+y_2+L_i)^2)^3}, \\ a^1_{21}(i) &= -2L_i\sigma_i\beta\frac{\tau(y_1+y_2+L_i)}{\pi(\tau^2+(y_1+y_2+L_i)^2)^2}, \\ a^2_{21}(i) &= 2L_i\sigma_i\beta^2 y_1y_2\frac{\tau(3(y_1+y_2+L_i)^2-\tau^2)}{\pi(\tau^2+(y_1+y_2+L_i)^2)^3}. \end{aligned}$$

These exact representations were used to test the numerical simulation based on the Karhunen-Loève expansions (46).

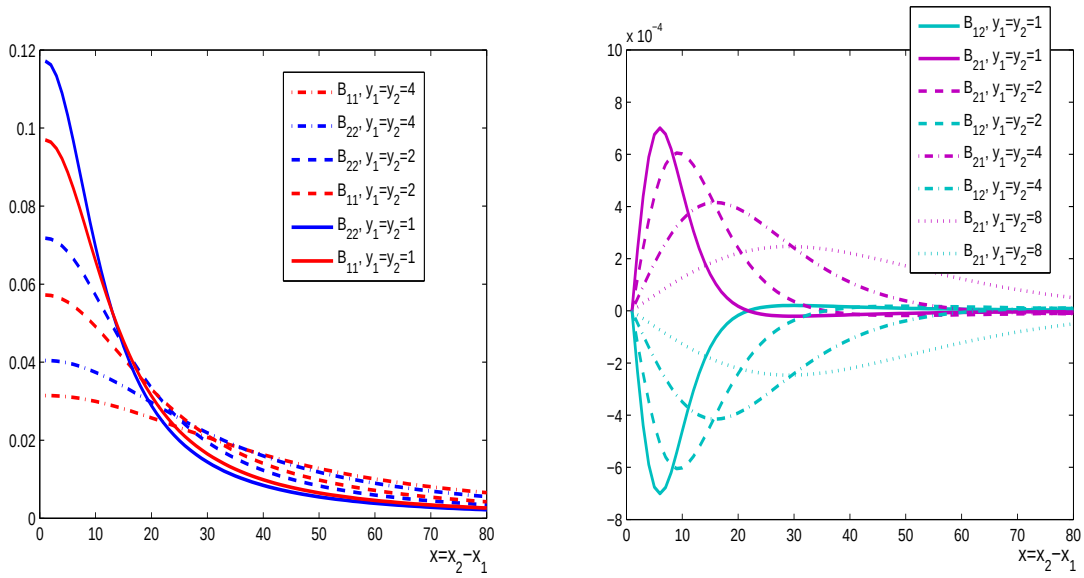

Figure 4: Boundary excitations with finite correlation lengths: the longitudinal B_{11} and transverse B_{22} correlation functions (left panel), and the cross-correlations B_{12} and B_{21} (right panel) versus the longitudinal coordinate x, for $\alpha = 1/3$, for different values of $y = y_1 = y_2$ and fixed correlation length $L_1 = L_2 = 1$.

Note that the relevant Karhunen-Loève expansion for the displacements for the considered example has the form

$$\mathbf{u}(x,y) \approx \frac{1}{\sqrt{R}} \sum_{k=1}^{\infty} e^{-\frac{\pi k y}{R}} S_g^{1/2}(\xi_k) \Big[\Big(\Re G_k(y)\, \zeta_k + \Im G_k(y)\, \eta_k \Big) \cos(\frac{\pi\, k\, x}{R}) + \Big(\Re G_k(y)\, \eta_k - \Im G_k(y)\, \zeta_k \Big) \sin(\frac{\pi\, k\, x}{R}) \Big] \,, \tag{49}$$

where $\xi_k = \pi k/R$, ζ_k and η_k are families of independent Gaussian vectors with zero mean and unit correlation matrix. From (47) we find the matrix $S_g^{1/2}(\xi_k)$ which is diagonal: $\{S_g^{1/2}(\xi_k)\}_{jj} = \sqrt{\sigma_j L_j}\, e^{-\xi_k L_j/2}$, $j = 1, 2$.

4.2 Simulation results for the finite correlation length boundary excitations.

In this section we analyse the correlation tensor for the example of finite correlation length excitations presented above by the expansions (46) and (49) and the exact expressions (48).

In Figure 4 we show how the correlation functions depend on the height y. We present the longitudinal B_{11} and transverse B_{22} correlation functions (left panel), and the cross-correlations B_{12} and B_{21} (right panel) versus the longitudinal coordinate x, for $\alpha = 1/3$, for different values of $y = y_1 = y_2$ and fixed correlation length $L_1 = L_2 = 1$. The results show clearly that with the height, the correlation length is increasing while the fluctuation intensity is decreasing. It should be noted that the elasticity constant α affects the behaviour of the curves very interesting. In Figure 5 we show the same curves as in Figure 4, but for $\alpha = \infty$. It is seen that for B_{22}, the intensity is increased about two times, with a little decrease of the correlation length.

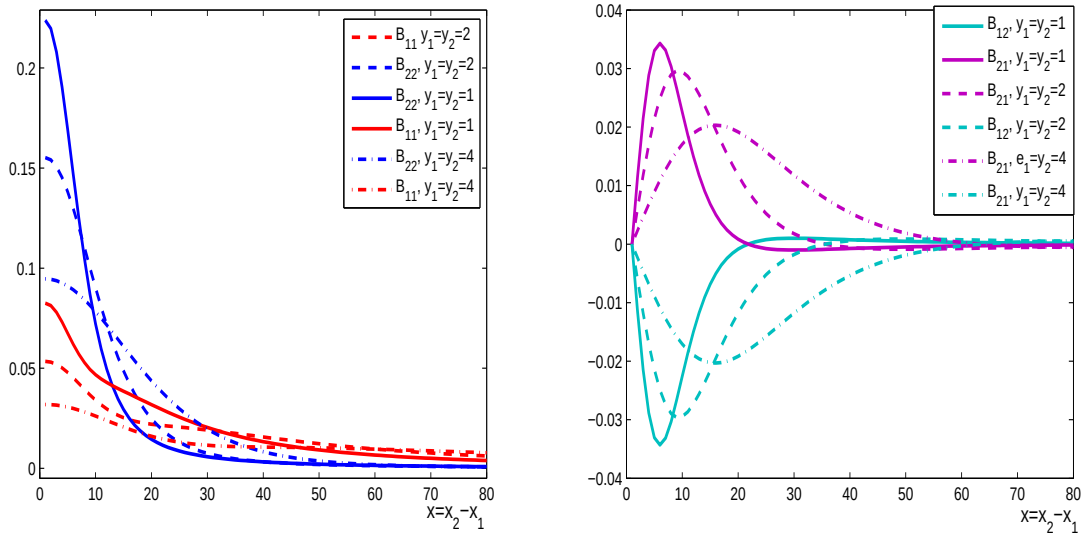

Figure 5: The same curves as in Figure 4, but for $\alpha = \infty$.

Remarkably, the correlation function B_{11} at $y_1 = y_2 = 1$ shows a kind of two characteristic correlation lengths behaviour.

In Figure 6 we analyze the dependence of the correlation functions on the input correlation lengths L_1 and L_2. Here we show the longitudinal B_{11} and transverse B_{22} correlation functions (left panel), and the cross-correlations B_{12} and B_{21} (right panel) versus the longitudinal coordinate x, for $\alpha = 2$, for different values of the correlation length L_1, and fixed $L_2 = 1$, at $y_1 = y_2 = 1$. From the results presented in the right panel it is seen that the change of the correlation length L_1 (L_2 fixed) affects only the correlations B_{11}, and does not influence the correlations B_{22}. In contrast, both B_{12} and B_{21} are quite sensitive to the change of L_1 (see the right panels of Figures 5 and 6 where L_2 was fixed at $L_2 = 1$).

Note that all the above functions were evaluated at fixed equal heights $y_1 = y_2$. It is seen from the exact formulae that the most height contributions come form $y_1 + y_2$, but in some cases also weighted by the product $y_1 y_2$, so it is interesting to analyze the correlation functions behaviour for different values of y_1 and y_2. In Figure 7 we show the correlation functions B_{11}, B_{22}, B_{12} and B_{21} versus x, for $\alpha = 222$, for different values of the heights, $y_1 = 0.5$, $y_2 = 2$, and different correlation lengths $L_1 = 0.1$, $L_2 = 1$ (left panel), and $L_1 = 1$, $L_2 = 1$ (right panel). It should be noted here that we plot $B_{12}(x, y_1, y_2)$ and $B_{21}(x, y_1, y_2)$, which are not antisymmetric, so $B_{12}(x, y_1, y_2) \neq -B_{21}(x, y_1, y_2)$ instead of the previous Figures where we had $B_{12}(x, y, y) = -B_{21}(x, y, y)$. We can see a drastic change in the correlation functions behaviour from the results presented in Figure 8 where we show the same curves as in Figure 7 but for different heights y_1, y_2 and different correlation lengths.

Finally let us consider the behaviour of the correlations as functions of the height y. In Figure 9 we plot the longitudinal B_{11} (dash lines) and transverse B_{22} (solid lines) correlations versus the transverse coordinate y, for 4 different values of $x = x_1 - x_2$: from up to down: $x = 1, 2, 3, 5$ for the correlation lengths $L_1 = L_2 = 1$ and $\alpha = 2$ (left panel), and the same curves for $\alpha = 222$ (right panel). From these curves it is seen that the increase of the longitudinal distance $x = x_1 - x_2$ leads to a rapid increase of the correlation length and a decrease of the fluctuation intensities. The same is true for the cross-correlations shown in Figure 10.

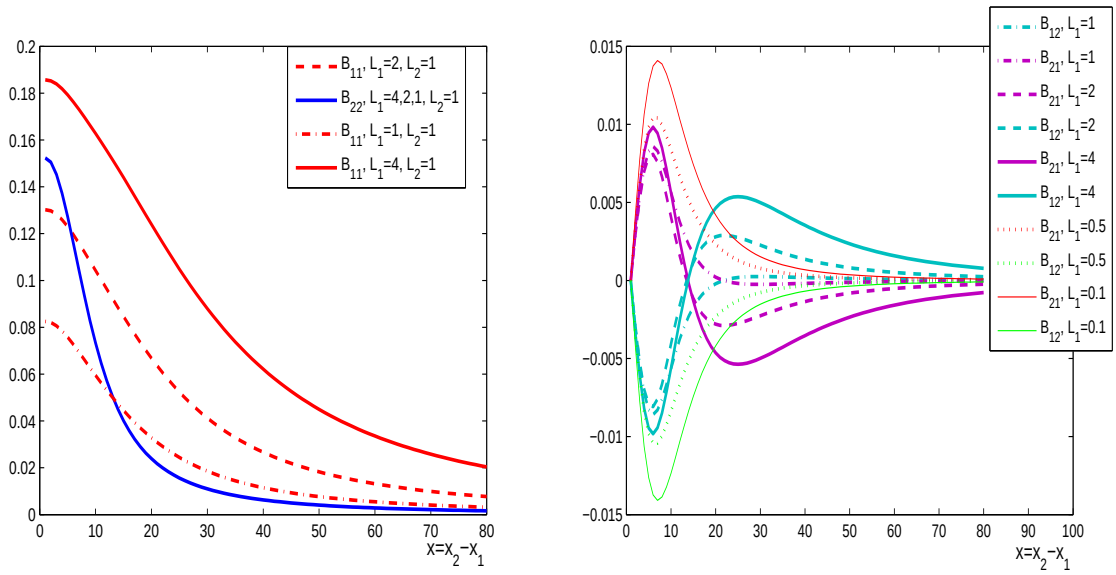

Figure 6: Boundary excitations with finite correlation lengths: the longitudinal B_{11} and transverse B_{22} correlation functions (left panel), and the cross-correlations B_{12} and B_{21} (right panel) versus the longitudinal coordinate x, for $\alpha = 2$, for different values of the correlation length L_1, and fixed $L_2 = 1$, at $y_1 = y_2 = 1$.

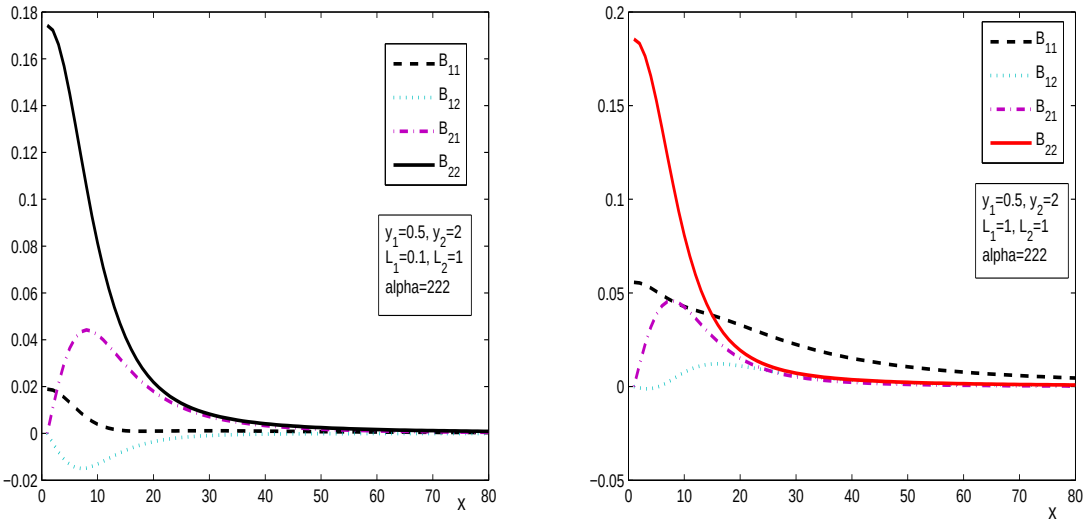

Figure 7: Boundary excitations with finite correlation lengths: the longitudinal B_{11}, transverse B_{22}, and the cross-correlations B_{12} and B_{21} versus the longitudinal coordinate x, for $\alpha = 222$, for different values of the heights, $y_1 = 0.5$, $y_2 = 2$, and different correlation lengths $L_1 = 0.1$, $L_2 = 1$ (left panel), and $L_1 = 1$, $L_2 = 1$ (right panel).

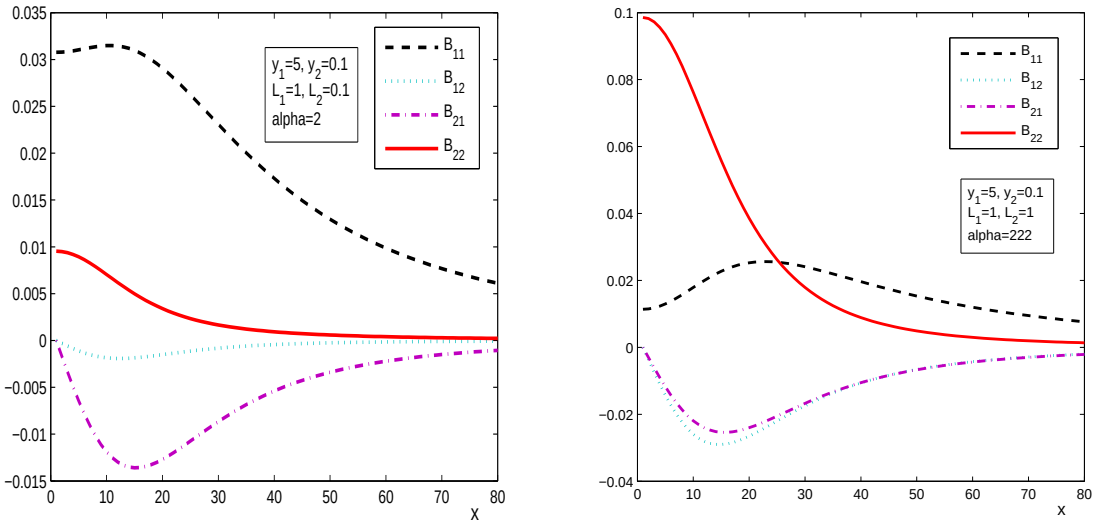

Figure 8: Boundary excitations with finite correlation lengths: the longitudinal B_{11}, transverse B_{22}, and the cross-correlations B_{12} and B_{21} versus the longitudinal coordinate x, for different values of the heights, $y_1 = 5$, $y_2 = 0.1$, for different correlation lengths $L_1 = 1$, $L_2 = 0.1$ and $\alpha = 2$ (left panel), and equal correlation lengths $L_1 = L_2 = 1$ and $\alpha = 222$ (right panel).

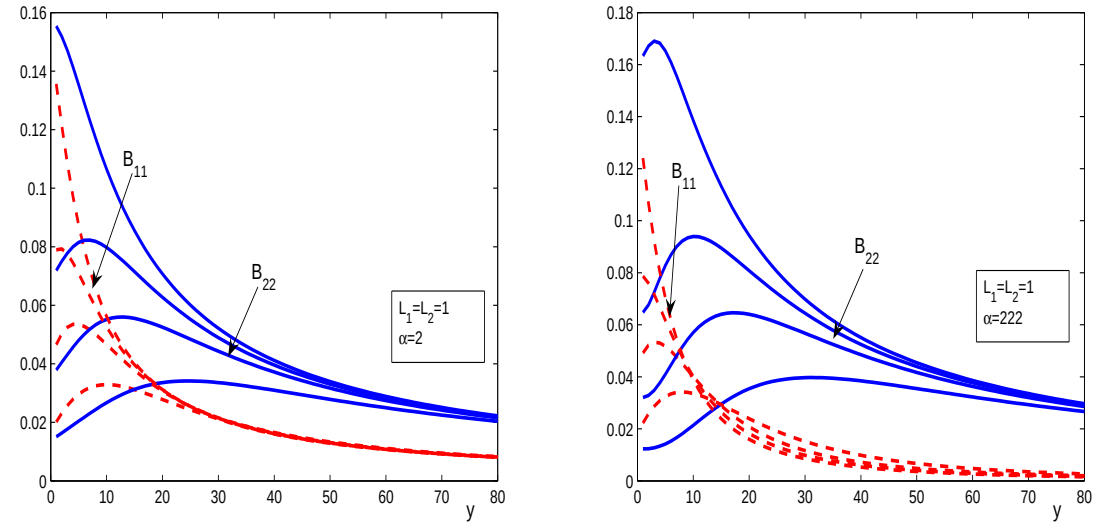

Figure 9: The longitudinal B_{11} (dash lines) and transverse B_{22} (solid lines) correlations versus the transverse coordinate y, for 4 different values of $x = x_1 - x_2$: from up to down: $x = 1, 2, 3, 5$ for the correlation lengths $L_1 = L_2 = 1$ and $\alpha = 2$ (left panel), and the same curves for $\alpha = 222$ (right panel).

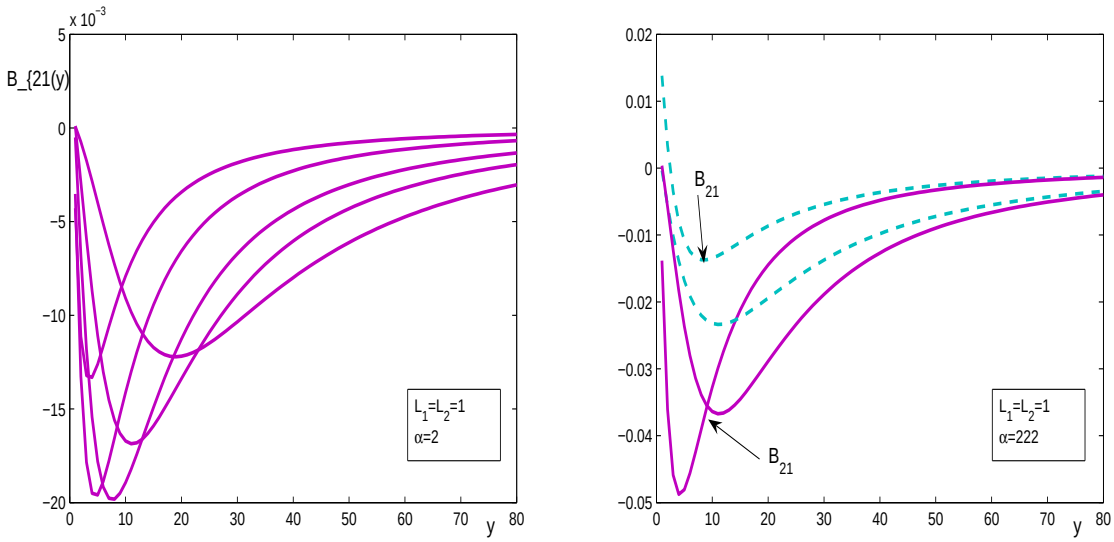

Figure 10: The same as in Figure 9, but for the cross-correlations B_{21} (left panel), for 5 different values of $x = x_1 - x_2$: from up to down along the tales of the curves: $x = 0.5, 1, 2, 3, 5$, for the correlation lengths $L_1 = L_2 = 1$ and $\alpha = 2$. In the right panel both B_{21} and B_{12} are shown for $x = 1$ and $x = 3$.

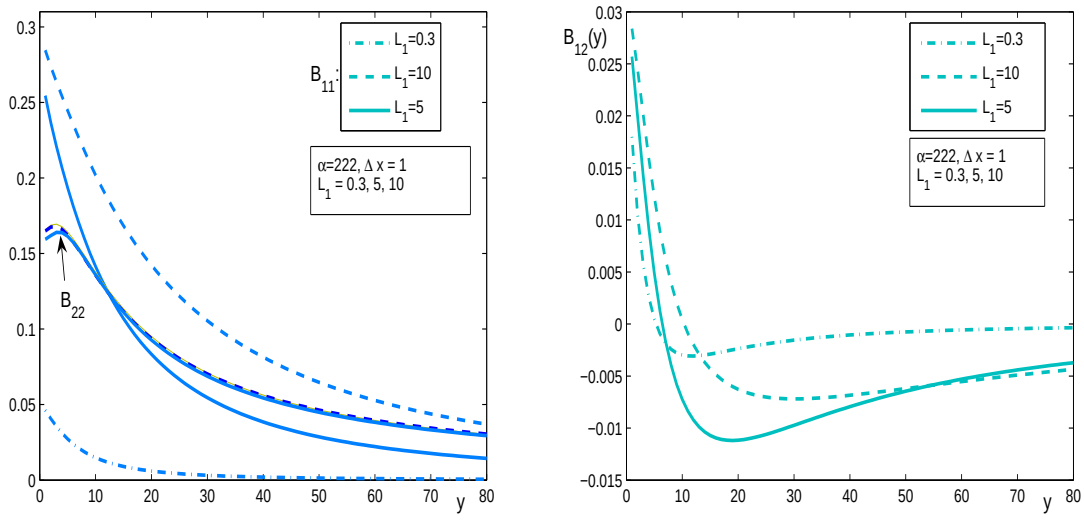

Figure 11: The longitudinal B_{11} and transverse B_{22} correlations versus the transverse coordinate y, for $\Delta x = x_1 - x_2 = 1$, for different values of the correlation length $L_1 = 0.3, 5, 10$, fixed $L_2 = 1$, and $\alpha = 222$ (left panel). It is clearly seen that the transverse correlations B_{22} are not affected by the change of the correlation length L_1. The relevant cross-correlations B_{12} are shown in the right panel.

In Figure 11 we present the longitudinal B_{11} and transverse B_{22} correlations versus the transverse coordinate y, for $\Delta x = x_1 - x_2 = 1$, for different values of the correlation length $L_1 = 0.3, 5, 10$, fixed $L_2 = 1$, and $\alpha = 222$ (left panel). It is clearly seen that the transverse correlations B_{22} are not affected by the change of the correlation length L_1. The relevant cross-correlations B_{12} are shown in the right panel.

Appendix: The Poisson formula for the upper half-plane

Let us denote by $\mathbf{U}(\xi, y) = (U_1(\xi, y), U_2(\xi, y))$ the inverse Fourier transform of the displacements $\mathbf{u}(x, y)$ over the variable x:

$$\mathbf{U}(\xi, y) = F^{-1}[\mathbf{u}(x, y)] = \frac{1}{2\pi} \int\limits_{-\infty}^{\infty} e^{-\imath x\xi} \mathbf{u}(x, y)\, dx \ .$$

If we apply the inverse Fourier transform to the system of Lam'e equation (1) we obtain the system

$$-(\lambda + 2\mu)\xi^2 U_1(\xi, y) + \mu \frac{\partial^2}{\partial y^2} U_1(\xi, y) + \imath(\lambda + \mu)\xi \frac{\partial}{\partial y} U_2(\xi, y) = 0$$

$$-\mu\xi^2 U_2(\xi, y) + (\lambda + 2\mu) \frac{\partial^2}{\partial y^2} U_2(\xi, y) + \imath(\lambda + \mu)\xi \frac{\partial}{\partial y} U_1(\xi, y) = 0 \ ,$$

here we use the simple property of the Fourier transformation

$$F^{-1}[D_x^\alpha u_i] = (\imath\xi)^\alpha F^{-1}[u_i] \ .$$

The solution of this system of ordinary differential for $y \geq 0$ is

$$U_1(\xi, y) = \big[(1 - \frac{\lambda + \mu}{\lambda + 3\mu}|\xi|y) U_1(\xi, 0) - \frac{\lambda + \mu}{\lambda + 3\mu} \imath\xi y U_2(\xi, 0)\big] e^{-|\xi|y}$$

$$U_2(\xi, y) = \big[(1 + \frac{\lambda + \mu}{\lambda + 3\mu}|\xi|y) U_2(\xi, 0) - \frac{\lambda + \mu}{\lambda + 3\mu} \imath\xi y U_1(\xi, 0)\big] e^{-|\xi|y} \ ,$$

where the vector $\mathbf{U}(\xi, 0)$ is the inverse Fourier transform of the boundary displacements $\mathbf{g}(x')$. Now we present every member in the right-hand side of last equations as the inverse Fourier transform, too. Now using simple Fourier transform formulae (e.g., see [6])

$$F^{-1}[\frac{y}{\pi(x^2 + y^2)}] = e^{-|\xi|y},$$

$$F^{-1}[\frac{x^2 - y^2}{\pi(x^2 + y^2)^2}] = F^{-1}[\frac{\partial}{\partial y}\big(\frac{y}{\pi(x^2 + y^2)}\big)] = -|\xi| e^{-|\xi|y},$$

$$F^{-1}[\frac{-2xy}{\pi(x^2 + y^2)^2}] = F^{-1}[\frac{\partial}{\partial x}\big(\frac{y}{\pi(x^2 + y^2)}\big)] = \imath\xi e^{-|\xi|y},$$

and the convolution property

$$F^{-1}[f * g] = F^{-1}[f] F^{-1}[g]$$

we get the desired result, the formula (2)

$$\mathbf{u}(x, y) = \int\limits_{-\infty}^{\infty} \frac{y\, Q(x - x', y)}{\pi((x - x')^2 + y^2)}\, \mathbf{g}(x')\, d\, x'$$

where the matrix Q is given by (3).

References

[1] Nadine Aubry. On the hidden beauty of the proper orthogonal decomposition. Theoretical and Computational Fluid Dynamics, **2** (1991), 339-352.

[2] G. Dagan. *Flow and Transport in Porous Formations*. Springer-Verlag, Berlin - Heidelberg, New York, 1989.

[3] Brian F. Farell, Petros J. Ioannou. Stochastic forcing of the linearized Navier-Stokes equations. Phys. Fluids A **5** (1993), N11, 2600-2609.

[4] Roger G. Ghanem, Pol D. Spanos. *Stochastic finite elements. A spectral approach.* Courier Dover Publications, 2003.

[5] Anthony Giordano and Michael Uhrig. Human face recognition technology using the Karhunen-Loeve expansion technique. Regis University. Denver, Colorado. http://www.rose-hulman.edu/mathjournal/archives/2006/vol7-n1/paper11/v7n1-11pd.pdf

[6] Gradstein, I.S. and Rygyk, I.M. *Tables of Integrals, Sums, Series and Products.* Nauka, Moscow, 1971 (in Russian).

[7] Huang S.P., Quek S.T., and Phoon K.K. Convergence study of the truncated Karhunen-Loeve expansion for simulation of stochastic processes. International Journal for numerical methods in engineering, **52** (2001), 1029-1043.

[8] I.F. Jones, S. Levy. Signal-to-noise ratio enhancememt in multichannel seismic data via the Karhunen-Loève transform. Geophysical Prospecting **35** (1987), N1, 12-32.

[9] Jari Kaipio, Ville Kolehmainen, Erkki Somersalo, and Marko Vauhkonen. Statistical inversion and Monte Carlo sampling methods in electrical impedance tomography. Inverse problems, **16** (2000), 1487-1522.

[10] V.M. Kaganer, R. Koeler, M. Schmidbauer, R. Opitz, and B. Jenichen. X-ray diffraction peaks due to misfit dislocations in heteroepitaxial structures. Physical Review B, vol. 55 (1997), N3, 1793-1810.

[11] Kolyukhin D. and Sabelfeld K. Stochastic flow simulation in 3D porous media. Monte Carlo Methods and Applications, **11** (2005), N1, 15-37.

[12] P. Kramer, O. Kurbanmuradov, and K. Sabelfeld. Comparative Analysis of Multiscale Gaussian Random Field Simulation Algorithms. Journal of Computational Physics, **226** (2007), 897-924.

[13] Kurbanmuradov O. and Sabelfeld K.K. Stochastic spectral and Fourier-wavelet methods for vector Gaussian random field. Monte Carlo Methods and Applications, **12**, N 5-6, 395-446.

[14] E.N. Lorenz. Empirical orthogonal functions and statistical weather prediction. Report 1, Statistical Forecasting Project, Massachusets Institute of technolohy, 1956.

[15] J.L. Lumley. The structure of homogeneous turbulent flows, in: Atmospheric Turbulence and Radio Wave Propagation, Edited by A.M. Yaglom and V.I. Tatarsky (Nauka, Moscow, 1967), p.166.

[16] A.S. Monin and A.M. Yaglom, *Statistical Fluid Mechanics: Mechanics of Turbulence*, The M.I.T. Press (1981), Vol. **2**.

[17] Obukhov, A.M., Statistical description of continuous fields. Tr. geophys. Int. Akad. nauk SSSR, **24** (1954), 3-42 (in Russian).

[18] J. Ophir, S. Alam, B. Garra et al. Elastography: Imaging the elastic properties of soft tissues with ultrasound. J. Med. Ultrasonics, **29** (2002), 155-171.

[19] Yu. A. Rozanov. F. Sanso. The analysis of the Neumann and the oblique derivative problem: the theory of regularization and its stochastic version. Journal of Geodesy, **75** (2001), 391-398.

[20] Sabelfeld, K.K. *Monte Carlo Methods in Boundary Value Problems.* Springer-Verlag, Berlin – Heidelberg – New York, 1991.

[21] Sabelfeld, K.K. Evaluation of elastic coefficients from the correlation and spectral tensors in respond to boundary random excitations. Proceed. Intern. Conference on Inverse and Ill-Posed pproblems of mathematical physics. dedicated to professor M.M. Lavrentiev on occation of his 75-th birthday. Novosibirsk, august 21-24, 2007.

[22] Sabelfeld K. and Kolyukhin D. Stochastic Eulerian model for the flow simulation in porous media. Monte Carlo Methods and Applications, **9** (2003), N3, 271-290.

[23] Sabelfeld, K.K. and Shalimova, I.A. *Spherical Means for PDEs.* VSP, The Netherlands, Utrecht, 1997.

[24] F. Sanso, G. Venuti. White noise stochastic BVP's and Cimmino's theory. PL da Vinci - IV Hotine-Marussi Symposium on Mathematical Geodesy: Trento, Italy, 2001, pp.5-20.

[25] M. Shinozuka, Simulation of multivariate and multidimensional random processes, J. of Acoust. Soc. Am. **49** (1971), 357-368.

[26] R. B. Sowers. Multidimensional reaction-diffusion equation with white-noise boundary perturbations. The Annals of Probability, **22** (1994), N 4, 2071-2121.

[27] D. Xiu and J. Shen. An efficient spectral method for acoustic scattering from rough surfaces. Communications in computational physics, **2** (2007), N 1, 54-72.

[28] X. Frank Xu. A multiscale stochastic finite element method on elliptic problems involving uncertainties. Computer Methods in Applied Mechanics and Engineering, **196** (2007), issues 25-28, 2723-2736.

[29] A.M. Yaglom. Correlation theory of stationary and related random functions I. Basic results. Springer-Verlag, New York - Heidelberg - Berlin, 1987.

[30] M.J. Yedlin, I.F. Jones, B.B. Narod. Application of the Karhunen-Loève transform to diffraction separation. IEEE Trans. acoust. speech signal Proc., Vol. ASSP-35 (1987), N 1, pp. 2-8.